Available online at www.sciencedirect.com
SCIENCE DIRECT®
C. R. Mecanique 331 (2003) 713–726
COMPTES RENDUS MECANIQUE

Concise Review Paper/Le point sur...

Near-critical fluid hydrodynamics

Bernard Zappoli [a,b]

[a] *CNES/HQ, 18, avenue E. Belin, 31401 Toulouse cedex, France*
[b] *IMFT, Université Paul Sabatier, 1, allée du Professeur Camille Soula, 31400 Toulouse, France*

Received 14 May 2003; accepted 19 May 2003

Article written at the invitation of the Editorial Board

Abstract

In the vicinity of the gas–liquid critical point, transport coefficients of pure fluids experience important changes. In particular, the thermal diffusivity tends to zero whereas the isothermal compressibility tends to infinity. Supercritical fluids are thus as dense as liquids and much more expandable than gases. These properties make the hydrodynamic similarity parameters vary over orders of magnitude when nearing the critical point, thus leading to a large field of research. We review here four main fields: heat transfer, cavity flows, interfaces and hydrodynamic instabilities. In the first, we present a fourth adiabatic heat transfer mechanism, called the piston effect, which carries heat much faster than diffusion, in the absence of convection. In the second, we show how this heat transfer mechanism interacts with buoyant convection. In the third, we basically show that a thermally non-homogeneous near-critical fluid behaves as a two miscible-phases fluid. In the fourth, we present some specific behavior of the Rayleigh–Benard convection, as recent experiments and numerical simulations have indicated. The last part gives some pathways in the continuation of the current research. We stress the need to fully develop the hydrodynamic of highly expandable, low heat diffusing fluids since the subject is both a bearer of new physics and is needed for the development of processes in chemical engineering. ***To cite this article: B. Zappoli, C. R. Mecanique 331 (2003).***
© 2003 Académie des sciences. Published by Éditions scientifiques et médicales Elsevier SAS. All rights reserved.

Résumé

L'hydrodynamique des fluides critiques. Les coefficients de transport des fluides purs présentent des variations importantes au voisinage du point critique liquide–gaz. En particulier, la diffusivité thermique tends vers zéro tandis que la compressibilité isotherme tend vers l'infini. Les fluides supercritiques sont donc aussi denses que des liquides et beaucoup plus compressibles que des gaz. Ces propriétés font varier de plusieurs ordres de grandeurs les paramètres de similitude lorsqu'on se rapproche du point critique ouvrant ainsi un champ de recherche très large. Nous faisons la synthèse de quatre principaux domaines : le transfert de chaleur, les écoulements de cavité, les interfaces et les instabilités hydrodynamiques. Dans le premier domaine nous présentons un quatrième mode de transfert de chaleur, dit par Effet Piston, qui transporte la chaleur beaucoup plus rapidement que par diffusion en l'absence de convection. Nous montrons dans le second comment ce mécanisme de transfert de chaleur interagit avec la convection. Dans le troisième domaine, nous montrons en fait qu'un fluide critique pur non homogène se comporte comme un fluide diphasique à phases miscibles. Nous présentons enfin quelques comportements spécifiques de la convection de Rayleigh–Benard comme les expériences et simulations numériques les ont récemment mis en évidence. La dernière partie donne quelques pistes pour la poursuite des travaux actuels. Nous insistons sur le besoin de développer complètement l'hydrodynamique des fluides très compressible et diffusant peu la chaleur car ce sujet est à la fois porteur de

E-mail address: bernard.zappoli@cnes.fr (B. Zappoli).

1631-0721/$ – see front matter © 2003 Académie des sciences. Published by Éditions scientifiques et médicales Elsevier SAS. All rights reserved.
doi:10.1016/j.crme.2003.05.001

physique nouvelle et nécessaire au développements du génie des procédés. ***Pour citer cet article : B. Zappoli, C. R. Mecanique 331 (2003).***
© 2003 Académie des sciences. Published by Éditions scientifiques et médicales Elsevier SAS. All rights reserved.

Keywords: Fluid mechanics; Gas–liquid critical point; Hydrodynamics

Mots-clés : Mécanique des fluides ; Point critique liquide–gaz ; Hydrodynamique

1. Introduction

When approaching the gas–liquid critical point (CP) of pure fluids, transport coefficients experience dramatic behavior. The heat conduction coefficient tends to infinity, the heat capacity at constant pressure tends to infinity, and the heat diffusivity is vanishingly small, while the isothermal compressibility diverges. Near critical fluids have been extensively studied as non-moving objects by physicists [1]. However, little still is known, compared to incompressible and normally compressible fluids, about the hydrodynamic behavior of these fluids since it lies between incompressible fluid mechanics and gas dynamics. The simpler situation of normally compressible non-Boussinesq fluids has not been extensively studied from the hydrodynamic point of view. For example, Spradley and Churchill [2] have studied pressure wave-driven (or thermoacoustic) motion which is generated by the local expansion of normally compressible fluids. Paolucci [3] has studied convection in strongly differentially heated cavities filled with normally compressible media. In addition to these studies of normally compressible media, a number of technical studies were devoted to the hydrodynamic behavior of very compressible cryogenic supercritical hydrogen or helium, which are known to be of great technological interest. For example, in the early 1970s, Heinmiller [4] has numerically studied convective flows in cryogenic tanks to describe the pressure collapse which follows a fast mechanical destratification of a near-critical fluid stored under microgravity conditions. In the field of hydrodynamic instabilities the situation is quite similar, although the theoretical works by Gitterman [5] and Spiegel [6] to obtain the stability criteria for supercritical fluid layers subjected the adverse temperature gradients must be cited first. Beyond these theoretical pioneering works, a number of experiments have been performed to explore organized fluid motion in the turbulent regime or on the route to turbulence in the Rayleigh–Benard heated-from-below configuration [7–18]. A number of key problems have been addressed, theoretically and experimentally. Global relations between the Nusselt number and others characteristic numbers, and more generally, scaling theory, large scale temperature fluctuations, pattern formation, spiral turbulence and random reversal of macroscopic flows are noteworthy. Besides these works inspired by the large variation of the similarity parameters when nearing the CP, we also review some very unique features not encountered in incompressible or normally compressible fluids obtained by real or numerical experiments: (i) a fourth heat transfer mechanism called the piston effect, which transfers energy on a time scale much shorter than any other, the apparent violation of the second principle of thermodynamics and the cooling of a heated critical fluids are examples of unexpected thermal behavior; (ii) a set of specific features in cavity flows: the isothermal convection, the inversion of acoustic waves reflection rules, the modification of boundary conditions by thermal adaptation layers, the solid body response to calibrated vibrations are presented as peculiarity of supercritical fluids cavity flows; (iii) the Rayleigh–Taylor-like instability in interface-free fluids; (iv) the thermoacoustic oscillations in the Rayleigh–Benard configuration. In the last section we give some ideas for future research in the field, including aspects linked to chemical engineering.

2. What is a critical fluid?

Any pure fluid which is set in thermodynamic equilibrium conditions above its critical point in the equilibrium phase diagram is called supercritical (see Fig. 1). When it is set very close and above the critical point it is usual to

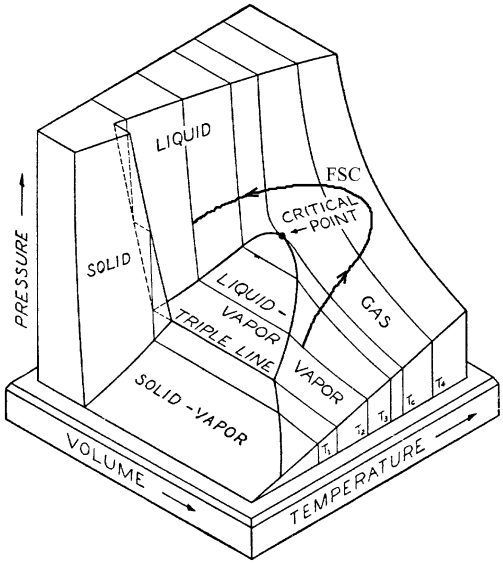

Fig. 1. The equilibrium phase diagram of a pure substance: the critical point is at the top of the liquid gas coexistence curve and the path indicated FSC shows that one can go continuously from gas to liquid in the supercritical region.

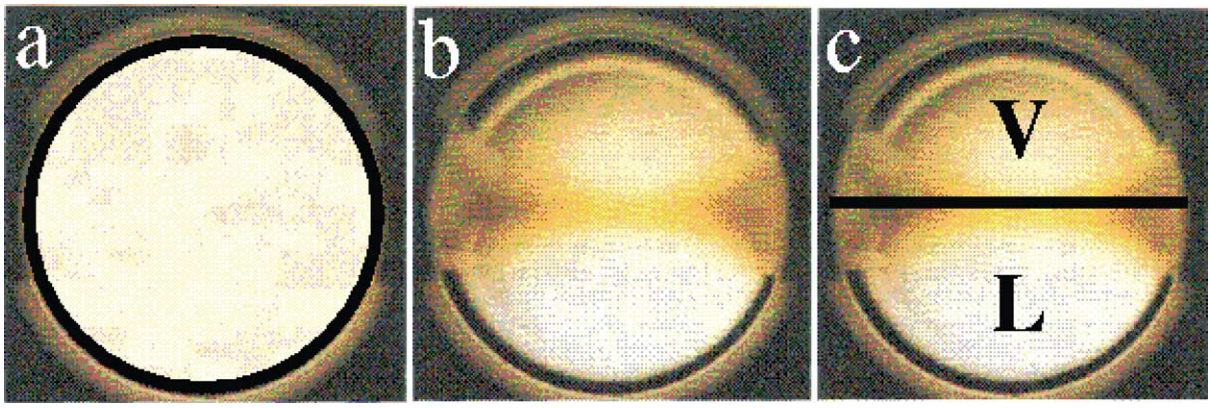

Fig. 2. Images of a cell filled at critical density with carbon dioxide above its critical temperature: (a) the fluid is one phase; (b) at critical temperature: density fluctuations make the fluid turbid in the middle of the cell where the critical density only is achieved because of the gravity stratification; (c) below the critical temperature: the interface between the liquid and the gas is planar and separates liquid from gas phases (from J. Straub).

say that the fluid is nearly supercritical. In particular, if we follow the path indicated on Fig. 1 it becomes possible to go continuously from the gas to the liquid phase without any phase transition.

For CO_2 the critical coordinates are $T_c = 304.13$ K, $\rho_c = 467.8$ kg·m^{-3}, $P_c = 7.376$ MPa. A supercritical fluid is thus a dense fluid since its density is half of that of water under normal conditions. Near the critical point the transport coefficients undergo dramatic behavior. The thermal expansion coefficient $\alpha_p = -(\partial\rho/\partial T)_p/\rho$, the isothermal compressibility $\chi_T = (\partial p/\partial\rho)_T/p$ and the isobaric specific heat C_p all strongly diverge as $\xi^{\gamma/\upsilon}$. The thermal diffusivity D_T decreases as ξ^{-1} while the shear viscosity is nearly constant. Here ξ is the thermal correlation length which growth as $\varepsilon^{-\upsilon}$ on the critical isochore with $\gamma \cong 1.24$ and $\upsilon \cong 0.625$ [1]. The Rayleigh number can thus be very large in the critical region, as large as 10^{13}, even for small size cavities ($L \leqslant 10$ cm); the

Prandtl number $Pr = \eta/\rho D_T$ is in the range 1–100. We should note that the isentropic compressibility diverges smoothly as $\varepsilon^{-0.11}$ and the speed of sound goes to zero with the same exponent. In brief, nearly supercritical fluids are dense fluids, highly heat conducting, deep heat reservoirs at constant pressure, poorly heat diffusing and highly expandable. The model, which is currently admitted for a supercritical fluid, is that of a Newtonian, viscous, heat conducting and highly expandable fluid. Its motion is thus described by the Navier–Stokes equations completed by an equation of state (EOS). The van der Walls (vdW) equation of state can give quite correct phenomenological description. The linearized EOS based on the expansion of pressure as a function of the independent thermodynamic variable leads to models aiming to compare with experimental results [19]. When the initial density is off-critical, the cubic model of the equation of state gives correct results, but we must take into account the variations of the transport coefficients with density [20]. It is also commonly admitted that the limit of validity of the Navier–Stokes model is reached when the smallest macroscopic length introduced by the description (thermal penetration length over the smallest time scale, for example) is equal or smaller than the correlation length. This limit is reached, at critical density, when the initial equilibrium temperature is closer to the critical one than some mK. When taking into account the critical anomalies, the following main characteristic features are found for supercritical fluids motion when nearing the CP: (i) the density perturbations in thermal dissipative layers diverge; and (ii) the power of the internal pressure stresses due to the deformation of any fluid element diverges.

3. Heat transport: the piston effect

As mentioned in the introduction, heat transport in nearly supercritical fluids was studied in the past, but the inadequacy of computational resources available at that time did not make it possible to identify the basic mechanisms. Following usual observations on the ground, very intense convective motion occurs in thermally non-homogeneous supercritical fluids. On the other hand, thermal transport measurements report on very fast heat transport although the heat diffusivity extremely small. It was thus proposed the idea that heat transport should be infinitely slow without convection be checked in the convection-free environment of space. In 1985, Straub [21] performed an experiment in a sounding rocket and found the bulk temperature to follow the wall temperature with a very short time delay. This meant that instead of observing a critical slowing down of the heat transport, Straub had observed an adiabatic critical speeding up, which was not interpreted as such at that time. No explanation was given until 1990 when three independent teams used different approaches to point out the thermo-compressive nature of the observed phenomenon. Onuki and Ferrel [22] used a purely thermodynamic approach and called the phenomenon ‘adiabatic effect’; Boukari and Gammon [23] used a semi-hydrodynamic method while Zappoli et al. [24] solved numerically the Navier–Stokes equations written for a van der Walls fluid. They called this speeding up ‘the piston effect’ since their approach permitted them to show the piston-like effect of the expanding fluid contained within the thermal boundary layer, which provokes mass addition in the bulk and thus an homogeneous increase in temperature.

After these initial theoretical approaches, many experiments were performed, as well as numerical and analytical studies. Experiments immediately faced the extreme instability of near-critical fluids on the ground [20] because of the diverging compressibility, which forced them to be conducted in the convection-free environment of space. Most of them were performed very close to the CP [25–29]. Moreover, when experiments are performed under microgravity conditions, the cell homogeneity is very difficult to attain during the available experimental times, because density inhomogenities relax on the divergently long thermal diffusion time [20]. In any case, the large value of thermal equilibration times in cell wall materials made ideal temperature steps very difficult to achieve, since the heat flux and the wall temperature are not well defined. To overcome these last difficulties, bringing energy to the fluid through an immersed thermistor, proved to allow for a good control of the heating parameters [19].

The analytical approach suffers from difficulties arising from the appearance of a third time scale, the one of heat transport, much shorter than diffusion and much longer than the acoustic one. Matching all the descriptions, both in space and time, is a technically difficult task [30].

The numerical solution of the Navier–Stokes equations faces the extremely large density gradients in thermal boundary layers which need a very robust description of fluxes at numerical cells boundaries [31]. The resulting computational time given by the finite volume formulation with an acoustic filtering procedure, even when using the SIMPLER algorithm, is very large.

Whatever the approach, the basic mechanism in a convection-free environment is the following. A very thin boundary forms when the wall is heated, owing to the very small heat diffusivity while the rest of the bulk fluid of length L remains non-affected by heat diffusion (isentropic). Since the heat diffusivity is very small, the characteristic heat diffusion time is very long and the bulk thus evolves at constant volume. It thus receives the energy $\Delta E_b = LC_V \Delta T_B$, where ΔT_B is the bulk increase in temperature. The boundary layer, in which pressure waves have time to smooth out pressure, receives the energy $\Delta E_{BL} = LC_p \Delta T_{BL}$. Temperature equilibration is reached when both bulk and boundary layer temperature variations are equal for the same energy variation. As $\delta = \sqrt{D_T t_{PE}}$ the characteristic time of the piston effect is $t_{PE} = t_{D_T}/\gamma^2$. The characteristic time of temperature equilibration tends to zero when nearing the critical point while the characteristic diffusion time tends to infinity. This effect has been studied by many teams to characterize the non-convective heat transfer, in terms of boundary effects [32], characterization of the relaxation after a heat pulse [19], non-convective coupling with the earth stratification [33]. The role of the micro-gravity environment has thus been to unmask the piston effect, which was disguised in convection on Earth. Some of its most remarkable properties are reported hereafter.

1. The piston effect is a thermoacoustic phenomenon. Acoustic compression waves are emitted, at heated boundaries, by thermal boundary layers, which provokes, when flashing back and forth in a container, a homogeneous increase of the bulk temperature. Fig. 3 illustrates this feature.

2. The piston effect is a fourth heat transport mechanism. Depending on boundary conditions the piston effect can transport heat from one side to another of a thermostated container on a very short time scale. Fig. 4 illustrates this feature. As the bulk phase is homogeneously heated by the piston effect, a boundary layer forms on the thermostated boundary, expansion acoustic waves are emitted which cool down the bulk phase, provoking a quick net heat transport from one side to the other of the cavity.

3. Temperature and density relaxations are uncoupled (at first order). After the piston effect has relaxed temperature, the fluid contained within the boundary layer cannot no longer expand; the remaining temperature inhomogeneities can thus only disappear by diffusion. As these very small inhomogeneities are associated to huge density gradients owing to the diverging compressibility, density relaxation seams to last for much longer than

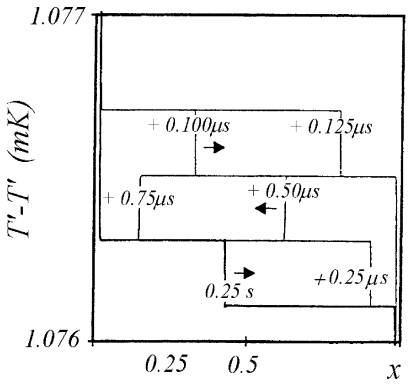

Fig. 3. The ‘painting effect’. Temperature in the sample after a boundary heating is shown on the acoustic time scale: each time the compression wave crosses the bulk it provokes an increase of temperature which has its specific time scale, much shorter than the heat diffusion time (reprinted from [34], with permission from Elsevier).

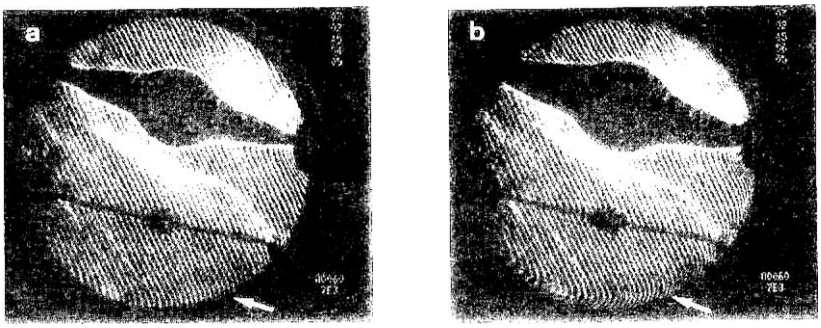

Fig. 4. Cooling boundary layer in CO_2 during a continuous heat supply through a thermistor (from [19]): (a) 4 s and (b) 5 s after the beginning of the heating. The straight fringes in the bulk of the figure indicate that the density is constant. The arrows show the deformation of the fringes close to the cell walls (which are maintained at the initial temperature which is 16.8 K above the critical temperature). The cooling boundary layer allows a net heat transport from the thermistor to the cell wall much faster than diffusion (published originally by the American Physical Society).

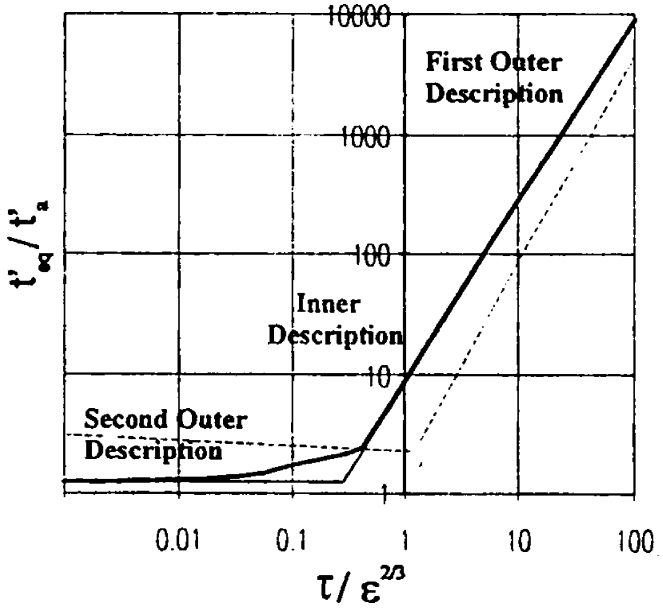

Fig. 5. The heat equilibration time as a function of the distance to the critical point (reprinted from [35] with permission of Elsevier): heat propagates at the speed of sound: when approaching the critical point closer than the cross over value, temperature is homogenized at the speed of sound. This is still to be checked experimentally.

the temperature relaxation. This is particularly important on the ground since convective instabilities have time to grow, since they are triggered by very long lasting density inhomogeneity [30].

4. Temperature can propagate at the speed of sound. When the critical point is approached closer than a cross-over value given by an asymptotic analysis, the piston effect characteristic time does not tend to zero monotonically but tends to a constant which is the characteristic acoustic time (Fig. 5). In CO_2 contained in a 10 mm long contained set at 1 K above its critical temperature, this cross over value is some mK. In these conditions, the temperature wave emitted by the thermal boundary layer has the same amplitude as the temperature increase at the wall [35].

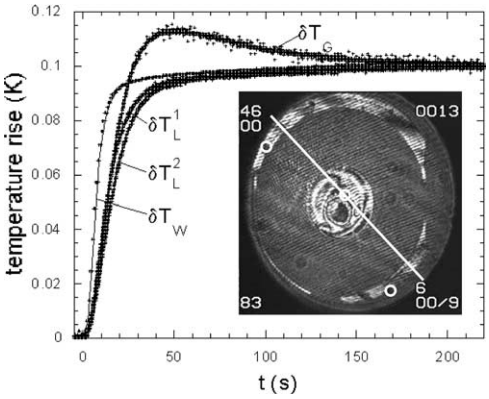

Fig. 6. Overheating observed during a 0.1 °C thermal quench in a cell filled with SF6 at 10 °C over the critical temperature: the gas temperature (δTG) is higher than that at the heating wall (δTL1, 2). Heat thus looks to flow from cold to hot (from [36], with permission from the authors; originally published by the American Physical Society).

Some striking behaviour due to the piston effect has been demonstrated by microgravity experiments. When heating a nearly sub-critical sample under microgravity conditions, the very compressible liquid, which is heated first since it wets the walls, compresses the gas phase. The gas phase properties are such that the temperature rise is more important than it is in the liquid. Heat thus seems to flow from cold to hot when not taking into account the piston effect (see Fig. 6) [19,37].

4. Cavity flows

As noted in the introduction, very little is known about cavity flows; some progress has recently been made in connection with the coupling of thermoacoustic and convective heat transport. After the importance of the piston effect on microgravity heat transport was recognized, the question which arose was to find the origin of the intense convective motion observed on the ground after a temperature rise at the boundary. In fact, if temperature is homogenized on a very short time scale why is the fluid experiencing hydrodynamic instabilities?: is the piston effect killed by convection, or is there another answer? It was shown [38] that the piston effect is not destroyed by convection and the density relaxation which occurs on the divergently long heat diffusion time scale, leaves time for a hydrodynamic instability to generate a convective motion in a quasi isothermal medium. Fig. 7 shows how different the convective structures can be in supercritical fluid compared to ideal gases.

Due to the extreme isothermal compressibility, the velocity of the fluid in the thermal boundary layer (see Fig. 7) is much higher than in the ideal gas. When the fluid reaches the upper wall there is a point where the velocity is zero (stagnation point) and thus where, according to conservation of energy, the fluid temperature increases by an amount corresponding to the kinetic energy gained during the rise along the heated wall. This is why the temperature of the upper wall can be higher than that of the heated wall, giving birth to the two-roll structure of the isothermal convection (Fig. 8).

In the case of the bulk heating of a sample, numerical simulations have demonstrated a thermal plume (Fig. 9). When its reaches an upper thermostated wall it generates a cooling boundary layer where a cooling piston effect takes place thus preventing any bulk increase of the temperature [38].

The triggering of the cold piston effect by the interaction of a hot fluid zone with a thermostated boundary was observed in [40], where it is shown that heating a boundary in the presence of an acceleration field can result in a cooling of the fluid, because of the cooling piston effect. More recently, this interaction has been shown

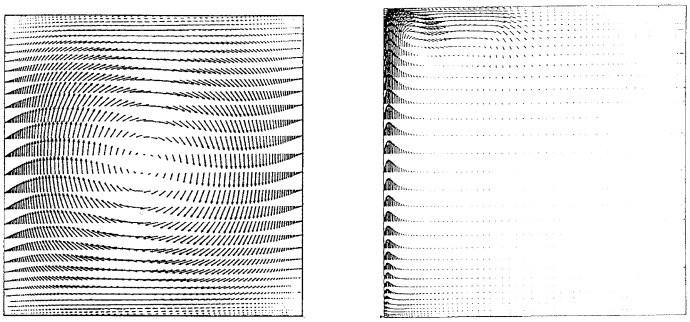

Fig. 7. Structure of the velocity field after the piston effect has homogenized temperature after a 1 mK increase in temperature at the left hand side wall (others are insulated): left, CO_2 when ideal gas; right, supercritical CO_2 (reprinted from [38] with permission from Cambridge University Press).

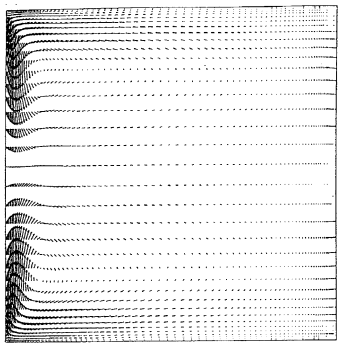

Fig. 8. Structure of the flow field on the heat diffusion time scale (about 10 min when the maximum velocity is still a thousand times higher that immediately after the heating in an ideal gas). The spot hotter than the left wall at the upper left corner generates a contra-rotative roll, which is isothermal convection-specific (reprinted from [38] with permission from Cambridge University Press).

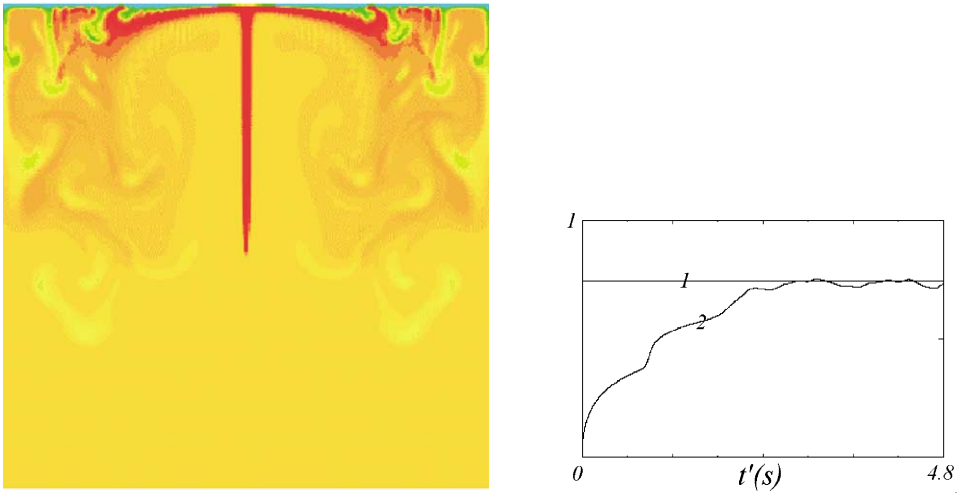

Fig. 9. Numerical simulation of the interaction of a thermal plume generated by a 5 mW heat flux through an immersed thermistor with the thermostated upper wall (left-hand side). Expansion acoustic waves are generated which equilibrate the constant input flux after a series of jumps correlated with the hydrodynamic events in the upper layer (left-hand side) (reprinted from [39] with permission from Cambridge University Press).

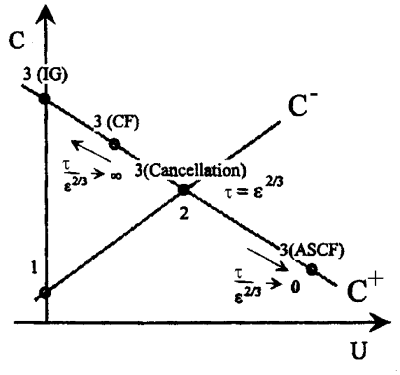

Fig. 10. Reflection of an incident acoustic wave on a closed thermostated end in the diagram fluid velocity (U)-velocity of sound (C). State 1 is the unperturbed state in which the wave propagates. State 2 is the fluid state behind the traveling wave. All the states (3) behind the reflected wave must satisfy boundary conditions: zero velocity at the wall (no adaptation layer) for an ideal gas (IG): the compression wave reflects as a compression wave. As the CP is neared, the flow towards the wall (velocity at the edge of the adaptation layer) is higher and higher and the wave reflects as an expansion wave (from [41], originally published by the American Institute of Physics).

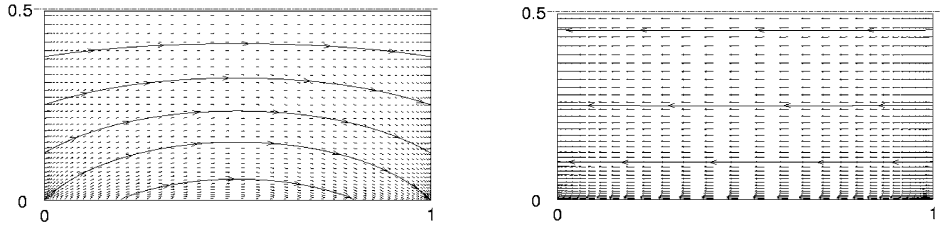

Fig. 11. The velocity field generated in micro-gravity conditions by a vibration the period of which is equal to the piston effect characteristic time. The presence of the adaptation layer homogenizes the velocity field in the supercritical fluid (right) while they are bent in the ideal gas (from [42], originally published by the American Institute of Physics).

to be responsible of thermal oscillations at the Rayleigh–Benard threshold (see the section on hydrodynamic instabilities).

Boundary conditions in compressible fluids drive the reflection of pressure waves on the wall, which bound the fluid domain. The presence of thermal adaptation layers strongly modifies the boundary conditions for the Navier–Stokes equations. In particular it changes the acoustic wave reflection rules. When a compression wave reaches a thermostated wall, the heated fluid generates a cooling adaptation layer in which the fluid is denser. Accordingly, a fluid flow is generated towards the wall. The incident wave does not see a closed end. Ultimately, following the theory of characteristics, (Fig. 10) it sees an opened end when closer than a certain distance from the critical point (which is exactly that of the cross-over to the acoustic saturation of the piston effect). It thus reflects as an expansion wave, apparently violating the reflection rule [41].

An example is given by a supercritical fluid, which is subjected to sinusoidal vibrations under zero g. When the period of the vibration is equal to the piston effect characteristic time, the velocity in the bulk is of the same order of magnitude as that at the edge of the adaptation layer. For this particular frequency, the thermoacoustic interaction has time to fully develop. As a consequence, the velocity in the bulk is quite homogeneous everywhere as in a solid (Fig. 11): the fluid bounces back and forth on the thermal boundary layers [42].

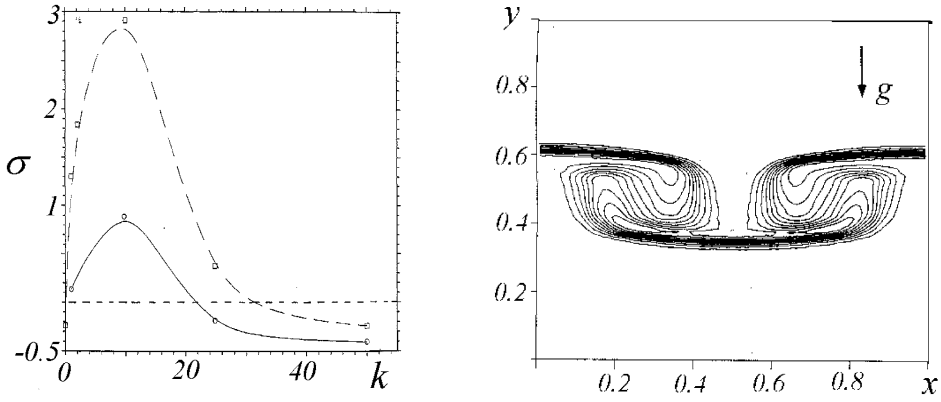

Fig. 12. Amplification coefficient as a function of the perturbation wave number from a numerical simulation (reprinted from [44] with permission from Elsevier): the dispersion curve for the Rayleigh–Taylor like instability between two different temperature supercritical fluid layers. As it is the case for miscible liquids and equilibrium interfaces, the dispersion curve exhibits cutoff and maximum amplification wave numbers.

5. Interfaces

When crossing the critical temperature, the interface between a critical isochoric liquid and its vapor disappears, to leave a very steep density gradient in a one-phase fluid. The question of the existence of a surface tension in such non-equilibrium interfaces is analogous to that of the existence of a surface tension between miscible liquids. In the case of miscible liquids, a Rayleigh–Taylor like instability at a miscible interface develops and the value of the most unstable wave-length is that of an equilibrium interface where the surface tension is replaced by the mass diffusivity [43]. In supercritical fluids, the thermal boundary layers are very thin because of the very low thermal diffusivity, while the density differences are much higher than in normal fluids because of the high isothermal compressibility. Thermal diffusivity drives the huge resulting density gradient in a similar way mass diffusivity drives density between miscible liquids. These thermal boundary layers which involve extremely steep density gradients may be considered as non-equilibrium interfaces which may develop instabilities as equilibrium interfaces. Of course, no surface tension is involved in a one-phase domain, but the existence of an equivalent surface tension can also be asked as it is asked for miscible liquids. In fact, it has been shown that a Rayleigh–Taylor like instability can be generated between two uniform layers of supercritical fluids at different temperature. Fig. 12 shows that the dispersion curve exhibits a cutoff wave length, the value of which can be correlated to that of miscible liquids, provided the species diffusion coefficient is replaced by the heat diffusion coefficient.

Not only should the interface behavior be questioned in the supercritical region, it also exhibits striking phenomena in the two-phase weakly sub-critical region. During the heating of the wall of a cell containing a two-phase near-critical fluid, the interface bends itself so that the vapor looks to wet the wall [45].

6. Hydrodynamic instabilities

In the past ten years, most attention has been devoted to fluid motion in organized structures forming in the Rayleigh–Benard configuration. Many works, the enumeration of which would go beyond the scope of the article, have been conducted in hydrodynamic instabilities in incompressible fluids such as water or mercury [46–48]. More recently, attention was paid, theoretically and experimentally, to the stability and the formation of organized structures in near-supercritical one-phase fluid layers. Essenheimer and Steinberg observed ‘target’ pattern states, initiated by defect-type instability in near supercritical SF_6 [17]. The properties of supercritical fluids also gave rise

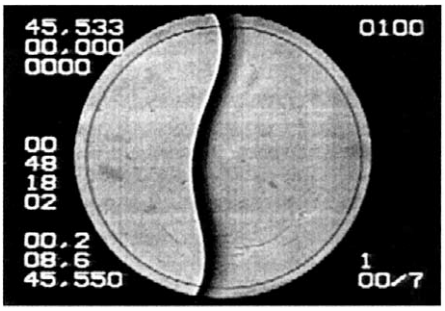

Fig. 13. The liquid de-wets the wall and the process is very similar to that occurring during the so called boiling crisis during which the liquid phase is isolated from the wall by a gas film. The origin of this drying process has shown to be due to the thrust of the vapor, which is produced in the vicinity of the liquid–vapor–solid triple contact line [45]. The only difference with the 'regular' boiling crisis in ideal fluids come from the fact that the interface deformation needs a much smaller force (very low interfacial tension) and thus a much smaller vapor production in near-critical fluids and the notion of critical heat flux has been introduced for near critical fluids as well (reprinted from [45] with permission from EDP Sciences).

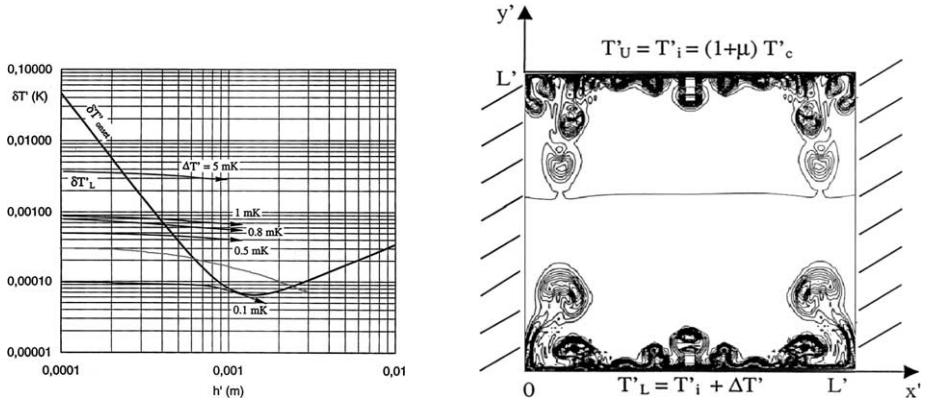

Fig. 14. As the piston effect heats up the bulk phase uniformly, a thermal adaptation layer forms at the top thermostated wall. This layer becomes unstable and gives the original double-instability pattern (right side). Moreover (left side), Rayleigh criteria (decreasing part of the curve) and Schwarzchild criteria (left hand side of the curve) are both accounted for (from [49,50]).

to unique features. Firstly, the transient states in cavities heated from below are strongly influenced by the piston effect which heat the bulk phase adiabatically, as shown by numerical simulations [49,50] (Fig. 14) or revealed by high precision measurements in ^{3}He [15] and well correlated with a recent numerical solution of approximated Navier–Stokes equations [51].

Secondly, the instability criteria usually given by the Raleigh criterion $Ra \geqslant Ra_c \cong 1708$ must be replaced by the a more general criterion which takes into account the fluid stratification [6], as in unconfined fluid column in atmospheric science. As the density decreases with height, the temperature gradient which destabilizes the fluid layer is lower than in incompressible fluids since the stability criteria becomes $Ra^{\text{corr}} = Ra(\alpha_p \rho g L^3/\eta D_T)(\Delta T - ATG) \geqslant Ra_c$ where standard notations are used. $ATG = L(\partial p/\partial T)_S \rho g$ is the adiabatic temperature gradient, e.g., the temperature gradient of a fluid particle, which rises adiabatically in the density gradient, as measured by Meyer et al. [14,15]. A review of the stability conditions is given by Gittermann [5]. The third peculiarity of near critical Rayleigh–Benard convection is that the experimental curve for $Ra(Nu - 1)$ versus Ra^{corr} for steady convective states are all located on a universal curve for different densities above T_c [15] and different values of the reduced distance to the CP on the isochore [14]. Furukawa and Onuki [51] have recently shown, for non-fully developed turbulence, that the universal function for the combination $Ra(Nu - 1)$ is given by $f_\lambda(Ra^{\text{corr}}, Pr)$ (as for

incompressible fluids for the same f_λ which is linked to the space-dependant temperature deviation from the linear gradient between the top and bottom surfaces). This law agrees well with experiments [9–11,14] which suggest, together with those by Allers and Xu [13], that f_λ is nearly independent of Pr for large values of this number. For higher values of the Rayleigh number, the expression $Nu \approx Ra^{1/4}(1 + C_1 Ra^b)$ where C_1 and b are of order 0.1 fit well with experimental data [12]. In their simulations, Furukawa and Onuki also find that when a rising eddy is strong enough to move through the cell, it can suppress the preexisting primary eddy and cause a global change in orientation (with at time period of about 50 s) as already noted by Niemela et al. for large enough Ra [16]. The last behavior we mention here is the large temperature fluctuations in Rayleigh–Benard cells observed by Kogan and Meyer [15]. Amiroudine and Zappoli showed by numerical experiment that they originate in the triggering of the cold piston effect at the upper, thermostated wall [52], a mechanism which was predicted numerically by Zappoli and Jounet in [39].

7. Future research

Near-supercritical fluid motion exhibits behaviors both belonging to gas dynamics and hydrodynamics since these dense fluids are strongly expandable. The exploration of cavity flows has shown new mechanisms, which basically are connected to the interaction between the piston affect and buoyant convection, and to energy propagation. Since this new behaviour is not yet checked experimentally, a first simple idea is to perform the corresponding experiments. Concerning the thermoacoustic aspect, the piston effect is a fourth heat transfer mechanism. It is able to carry heat independently of distance in a way faster than all the other known mechanisms. R and T work must be conducted to develop the feasibility of a piston effect-based heat pipe, to cool down either 3D new generation electronic components or micro thermodynamic devices.

Behaviour under vibrations, either rotational or not, with or without gravity, certainly contains potential new physics. In this field there are strong needs to develop new averaged formulation of the equations since direct numerical simulation (DNS) performed until now have proven the computational time to be extremely long. Beyond the cavity flow problem is the extension to near critical fluids of all the classical problems of aerodynamics, gas dynamics or hydrodynamics. Nothing yet is known, even theoretically, about the effect of shear flow energy dissipation in dynamical boundary layers, for example, or on the way to handle pipe flows or nozzle flows, either isentropic or not, steady or unsteady. High speed supercritical fluid flow studies could also be pursued in continuation of those performed in the 1980s on the rarefaction shock wave formation [53–55]. For low Reynolds number flows, theses questions become micro-hydrodynamics and are linked to extremely important technical problems such as cryogen tank leakage or high pressure flows in porous media.

Narrow heat diffusion layers, in which huge density gradients drive hydrodynamic instabilities in a similar way to a concentration gradient in miscible liquids, replace interfaces in the supercritical region. Apart from the results presented in this review, nothing is known on the evolution of the cutoff frequency, for example, as a function of the initial layer thickness, and of the overall stability conditions in the Rayleigh–Taylor configuration. Although some work has been performed on the Rayleigh–Benard instability, the role of vibrations on the threshold location and its existence is still unknown. 3D target-like pattern formation is also still a challenge for DNS.

A natural extension of these topics is to chemical engineering. In fact, supercritical fluids are already of interest for their solvent properties and the possibility for chemical reaction to come to completion at a much lower temperature, in supercritical water, for example. However, very little is theoretically known about supercritical chemical hydrodynamics and models are often very crude and need improvement [56,57]. Well-defined model systems representative of some basic problem such as transport at the solid-supercritical mixture interface should be build up experimentally and theoretically. Dilution of naphthalene in supercritical carbon dioxide in the vicinity of the lower end critical point (where the triple line of the mixture meets its critical line) will certainly reveal new striking behaviour linked to the diverging osmotic pressure such as the speeding up of mass transport. The extension of classical combustion model problems such as the Emmons problem (flat plate combustion) or droplet

combustion should also lead to original, extremely important issues for rocket propulsion and hydrogen clean combustion.

References

[1] H.E. Stanley, Introduction to Phase Transitions and Critical Phenomena, Clarendon Press, Oxford, 1971.
[2] L.W. Spradley, S.W. Churchill, J. Fluid Mech. 70 (1975) 705.
[3] S. Paolucci, Sandia NAti. Lab. SAND 82-8257, 1982.
[4] P.J. Heinmiller, TRW Rep. 17618-H080-R0-00, Houston, USA.
[5] M. Gittermann, Rev. Mod. Phys. 50 (1978) 85.
[6] E.A. Spiegel, Int. Astrophys. J. 141 (1965) 1068.
[7] M. Sano, X.-Z. Wu, A. Libshaber, Phys. Rev. A 40 (1989) 6421.
[8] X.-Z. Wu, A. Libshaber, Phys. Rev. A 45 (1992) 842.
[9] S. Ashkenazi, V. Steinberg, Phys. Rev. Lett. 83 (1999) 3641.
[10] X. Chavanne, F. Chilia, B. Castaing, B. Hebral, B. Chabaud, J. Chaussy, Phys. Rev. Lett. 79 (1997) 3648.
[11] W. Chavanne, Ph.D. Thesis, Univ. Joseph Fourrier, Grenoble, 1997.
[12] X. Xu, K.M.S. Bajaj, G. Allers, Phys. Rev. Lett. 84 (2000) 4357.
[13] G. Allers, X. Xu, Phys. Rev. Lett. 86 (1999) 3320.
[14] A.B. Kogan, D. Murphy, H. Meyer, Phys. Rev. Lett. 82 (1999) 4635.
[15] A.B. Kogan, H. Meyer, Phys. Rev. E 63 (2001) 056310.
[16] J.J. Niemela, L. Skrbek, K.R. Sreenivasan, R.J. Donnelly, Nature (London) 404 (2000) 837.
[17] J.J. Niemela, L. Skrbek, K.R. Sreenivasan, R.J. Donnelly, J. Fluid. Mech. 449 (2001) 169.
[18] M. Assenheimer, V. Steinberg, Phys. Rev. Lett. 70 (1993) 3888.
[19] Y. Garrabos, M. Bonetti, D. Beysens, F. Perrot, T. Fröhlich, P. Carlès, B. Zappoli, Phys. Rev. E 57 (1998) 5665.
[20] J.V. Sengers, J.M.H. Levelt Sengers, in: C.A. Croxton (Ed.), Progress in Liquid Physics, Wiley, New York, 1978, references therein.
[21] K. Nitsche, J. Straub, in: Proc. Sixth Europ. Symp. on Mat. Sc. under Micro-g Conditions, Bordeaux, France, 1986, p. 109. ESA, SSP-256.
[22] A. Onuki, H. Hao, R.A. Ferrel, Phys. Rev. A 41 (1990) 2256–2259.
[23] H. Boukari, J.N. Saurneyer, M.E. Briggs, R.W. Gammon, Phys. Rev. A 41 (1990) 2260–2263.
[24] B. Zappoli, D. Bailly, Y. Garrabos, B. Le Neindre, P. Guenoun, D. Beysens, Phys. Rev. A 41 (1990) 2264–2267.
[25] M.R. Moldover, J. Sengers, R.W. Gammon, R.J. Hocken, Rev. Mod. Phys. 51 (1979) 79.
[26] H. Boukari, M.E. Briggs, J.N. Shaurneyer, R.W. Gammon, Phys. Rev. Lett. 65 (1990) 2654.
[27] H. Klein, G. Schmitz, D. Woerman, Phys. Rev. A 43 (1991) 4562.
[28] P. Guenoun, B. Khalil, D. Beysens, Y. Garrabos, F. Kamoun, B. Le Neindre, B. Zappoli, Phys. Rev. E 47 (1993) 1531.
[29] J. Straub, L. Eicher, A. Haupt, Phys. Rev. E 51 (1995) 5556.
[30] D. Bailly, B. Zappoli, Phys. Rev. E 62 (2000) 2353.
[31] S. Amiroudine, J. Ouazzani, B. Zappoli, P. Carlès, Eur. J. Mech. B Fluids 16 (1997) 665.
[32] R.A. Ferrel, H. Hao, Physica A 197 (1993) 23.
[33] H. Boukari, R.L. Pego, R.W. Gammon, Phys. Rev. E 52 (1995) 1614.
[34] B. Zappoli, P. Carles, Eur. J. Mech. B Fluids 14 (1995) 1.
[35] B. Zappoli, P. Carles, Physica D 89 (1995) 381.
[36] R. Wunenbuerger, Y. Garrabos, C. Lecoutre-Chabot, D. Beysens, J. Hegseth, Phys. Rev. Lett. 84 (2000) 4100.
[37] “Vibrating Grains Form Crumps”, Science News 156 (17.7.99).
[38] B. Zappoli, S. Amiroudine, P. Carles, J. Ouazzani, J. Fluid Mech. 316 (1996) 53.
[39] B. Zappoli, A. Jounet, S. Amiroudine, A. Mojtabi, J. Fluid Mech. 388 (1999) 389.
[40] T. Fröhlich, Ph.D. Thesis, Munich, 1997.
[41] B. Zappoli, P. Carles, S. Amiroudine, J. Ouazzani, Phys. Fluids 7 (1995) 2283.
[42] A. Jounet, A. Mojtabi, J. Ouazzani, B. Zappoli, Phys. Fluids 12 (2000) 197–204.
[43] P. Kurowski, C. Misbah, S. Tchoukine, Eur. Phys. Lett. 29 (1995) 309.
[44] B. Zappoli, S. Amiroudine, S. Gauthier, C. R. Acad. Sci. Paris, Sér. IIb (1997) 1–6.
[45] V. Nikolayev, D. Beysens, Europhys. Lett. 47 (1999) 345.
[46] B.J. Gluckman, H. Willaime, J.P. Gollub, Phys. Fluids A 5 (1993) 647.
[47] S. Cioni, S. Ciliberto, J. Sommeria, J. Fluid. Mech. 335 (1997) 111.
[48] E.D. Siggia, Annu. Rev. Fluid Mech. 26 (1994) 137.
[49] S. Amiroudine, P. Bontoux, P. Larroudé, B. Gilly, B. Zappoli, J. Fluid Mech. 442 (2000) 119.
[50] L.E. Khouri, P. Carlès, Phys. Rev. E 66 (2002) 066309.

[51] A. Furukawa, A. Onuki, Phys. Rev. E 66 (2002) 016302.
[52] S. Amiroudine, B. Zappoli, Phys. Rev. Lett. 90 (2003) 105303.
[53] A.A. Borisov, S.S. Kutateladze, V.E. Nakoryalov, J. Fluid. Mech. 126 (1983) 59.
[54] P.A. Thomson, K.C. Lambraki, J. Fluid. Mech. 60.
[55] M.S. Kramer, A. Kluwick, J. Fluid. Mech. 142.
[56] T.J. Bruno, J.F. Ely, Supercritical Fluids Technology. Review in Modern Theory and Applications, CRC Press, Boca Raton, 1991.
[57] F.V. Bright, M.P.E. McNally, Supercritical Fluids Technology. Theoretical Approaches in Analytical Chemistry, ACS Symp. Ser., Vol. 488.